Hindawi Publishing Corporation
BioMed Research International
Volume 2015, Article ID 138060, 9 pages
http://dx.doi.org/10.1155/2015/138060

Research Article

Optimal Experiment Design for Monoexponential Model Fitting: Application to Apparent Diffusion Coefficient Imaging

Mohammad Alipoor,[1] Stephan E. Maier,[2] Irene Yu-Hua Gu,[1] Andrew Mehnert,[3] and Fredrik Kahl[1]

[1]*Department of Signals and Systems, Chalmers University of Technology, 41296 Gothenburg, Sweden*
[2]*Department of Radiology, Sahlgrenska University Hospital, Gothenburg University, 41345 Gothenburg, Sweden*
[3]*Centre for Microscopy, Characterisation and Analysis, The University of Western Australia, Perth, WA 6009, Australia*

Correspondence should be addressed to Mohammad Alipoor; alipoor@chalmers.se

Received 11 September 2015; Accepted 6 December 2015

Academic Editor: Guang Jia

The monoexponential model is widely used in quantitative biomedical imaging. Notable applications include apparent diffusion coefficient (ADC) imaging and pharmacokinetics. The application of ADC imaging to the detection of malignant tissue has in turn prompted several studies concerning optimal experiment design for monoexponential model fitting. In this paper, we propose a new experiment design method that is based on minimizing the determinant of the covariance matrix of the estimated parameters (D-optimal design). In contrast to previous methods, D-optimal design is independent of the imaged quantities. Applying this method to ADC imaging, we demonstrate its steady performance for the whole range of input variables (imaged parameters, number of measurements, and range of b-values). Using Monte Carlo simulations we show that the D-optimal design outperforms existing experiment design methods in terms of accuracy and precision of the estimated parameters.

1. Introduction

The monoexponential model has been used in many different engineering applications. It is frequently used in modeling biomedical phenomena to estimate biologically meaningful parameters. Its applications in quantitative biomedical imaging include apparent diffusion coefficient (ADC) imaging [1], monitoring metabolic reactions [2], and pharmacokinetics [3]. ADC imaging has a wide range of applications including the classification of brain disorders [4], detection of malignant breast lesions [5], identifying stages of cerebral infarction [6], and diagnostic imaging of the kidney [7, 8], prostate [9, 10], and ovaries [11, 12]. ADC imaging is also used to solve challenging clinical problems such as the differentiation of Parkinson's disease from multiple system atrophy and progressive supranuclear palsy [13].

The usefulness of ADC imaging as a quantitative imaging tool has motivated several studies that have investigated the reliability and reproducibility of ADC estimates [7, 14, 15]. From a mathematical point of view, the variance of the estimated ADC values can be minimized by optimizing experiment design. In the case of ADC imaging, experiment design equates to the choice of the b-values applied for measurements and their repetitions. In the case of enzyme kinetics, it equates to the sample collection time (t). The range of valid sampling points is determined by the biophysical aspects of the problem at hand. For instance, perfusion contamination at low b-values [15, 16] and SNR drop at high b-values [1] limit the applicable range of b-values. An intuitively appealing experiment design is the equidistant (ED) distribution of sampling points on a valid range of the independent variable (b or t). The ED experiment design method is widely used in the literature [7, 17–19]. However, many studies use nonsystematic and random experiment designs [9, 20] that can considerably influence the results.

Some studies have tried to find the optimal experiment design by empirically evaluating a variety of experiment designs [17]. In contrast, others have developed a theoretical

framework by minimizing the variance of the estimated parameters [21–23]. The former strategy may potentially miss the global optimum because of the discretization of the problem and a nonexhaustive search. On the other hand, studies pursuing the latter strategy are based on the Gaussian noise assumption. The Cramer-Rao lower bound (CRLB) of the ADC value is minimized in [23] assuming a Gaussian noise distribution. Hereinafter, we call this method GCRLB. The optimal experiment design in the GCRLB method (briefly described in Appendix B) depends on the ADC values to be imaged. Thus the optimal design must be revised for different applications and even for imaging different organs. Moreover, in applications where the noise assumption is violated, the GCRLB design becomes suboptimal. In this paper, we develop a theoretical framework for optimal experiment design of monoexponential model fitting problems with less restrictive assumptions on noise distribution. Our Monte Carlo simulations using the proposed design method for ADC imaging show that, in the presence of Rician noise, it outperforms the GCRLB and ED methods. In addition, the proposed design is independent of the imaged parameters and provides more robust results.

The remainder of the paper is organized as follows. The next section elaborates the proposed experiment design method. Section 3 presents results of extensive evaluations and comparisons. A discussion of different aspects and the potential impact of this work is given in Section 4. Finally the conclusion is presented in Section 5.

2. Proposed Experiment Design Method

Without loss of generality, hereinafter we focus on ADC imaging as an example of monoexponential model fitting problems. The model for ADC imaging is given by

$$m = m_0 \exp(-bD), \tag{1}$$

where m is the measured signal when the diffusion weighting factor b is applied, m_0 is the observed signal in the absence of such a weighting factor, and D is the apparent diffusion coefficient. The parameters to be estimated are m_0 and D. In ADC imaging the parameter of interest is D. However, there exist applications in which m_0 is also important such as (6) in [2]. Although mathematically two measurements suffice, in practice $N > 2$ measurements are acquired to maximize precision. Depending on the problem at hand, one is permitted to choose the independent variable (b in this case) such that $b_{\min} \le b \le b_{\max}$. Log-linear least square fitting is frequently used because of its computational efficiency [18]. It can be formulated as follows:

$$\ln m_i = \ln m_0 - b_i D, \quad \forall i = 1, \ldots, N. \tag{2}$$

For N measurements we obtain

$$\mathbf{y} = \mathbf{A}\mathbf{x}, \tag{3}$$

where $\mathbf{y} \in \mathbb{R}^N$ contains measurements ($\ln m_i$), $\mathbf{x} \in \mathbb{R}^2$ contains unknown parameters ($\mathbf{x} = [\ln m_0 D]^T$), and $\mathbf{A}$ is the design matrix below:

$$\mathbf{A} = \begin{bmatrix} 1 & -b_1 \\ \cdots & \cdots \\ 1 & -b_N \end{bmatrix}. \tag{4}$$

The least squares estimator (LSE) of $\mathbf{x}$ is given by $\hat{\mathbf{x}} = (\mathbf{A}^T\mathbf{A})^{-1}\mathbf{A}^T\mathbf{y}$. The precision of the estimation problem above is dependent on the experiment design $\mathbf{A}$. For independent and zero-mean measurement noise (on $\mathbf{y}$) with constant variance σ^2 the LSE is unbiased and has the following covariance matrix [24]:

$$\mathrm{Cov}(\hat{\mathbf{x}}) = \sigma^2 \mathbf{M}^{-1}, \tag{5}$$

where $\mathbf{M} = \mathbf{A}^T\mathbf{A}$ and is usually called the "*information matrix*." Optimal experiment design entails making the covariance matrix *small* in some sense. It is usual to minimize a scalar function of the covariance matrix. One design approach is to minimize the determinant of the information matrix (D-optimal design). In this paper, we solve the D-optimal experiment design problem for ADC imaging.

Remark 1. The noise distribution on the diffusion attenuated signal (denoted by m) is usually assumed to be Rician. To investigate the significance of our noise assumptions in the case of ADC imaging, we use Monte Carlo simulations. Let $|m + w|$ model the measured diffusion signal, where m is the true value of the signal and $w = w_R + jw_I$ is the complex-valued measurement noise. The noise components are Gaussian distributed: $w_R \sim \mathcal{N}(0, \sigma_G^2)$, $w_I \sim \mathcal{N}(0, \sigma_G^2)$. We perform Monte Carlo simulations with Rician noise (on m) and the following setup: number of Monte Carlo trials $N_{\mathrm{MC}} = 20000$, $\sigma_G = 20$, and m varies from 5 to $20\sigma_G$ with equal step size of 5. As can be seen in Figure 1, the zero-mean assumption (on $y_i = \ln m_i$) holds for SNR > 2 while the equal variance on log-measurements ($\mathbf{y}$) holds for SNR > 10. Overall, this shows that both zero-mean and equal variance assumptions hold for SNR > 10. Thus, we expect the proposed method to have diminished performance for high b-values and high D values.

2.1. D-Optimal Experiment Design for Monoexponential Model Estimation. The D-optimal experiment design is based on minimizing the determinant of the covariance matrix of the LSE. The D-optimal experiment design for ADC imaging can be written as follows:

$$\begin{aligned} &\min \quad \det\left(\mathbf{M}^{-1}\right) \\ &\text{s.t.:} \quad \mathbf{M} \ge 0, \\ &b_{\min} \le b_i \le b_{\max}, \quad i = 1, \ldots, N, \end{aligned} \tag{6}$$

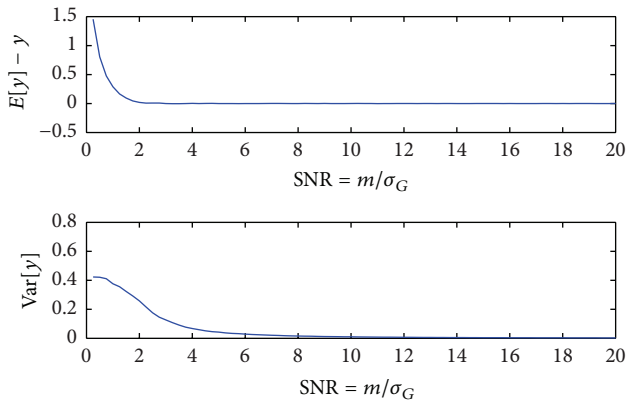

Figure 1: Results of Monte Carlo simulations show that if SNR > 10, then zero-mean and equal variance noise assumptions hold for ADC imaging. Simulation setup: number of Monte Carlo trials $N_{\mathrm{MC}} = 20000$, $\sigma_G = 20$, and m varies from 5 to $20\sigma_G$ (equal step size of 5).

where the explicit expression for $\mathbf{M}$ is

$$\mathbf{M} = \begin{bmatrix} N & -\sum_{i=1}^{N} b_i \\ -\sum_{i=1}^{N} b_i & \sum_{i=1}^{N} b_i^2 \end{bmatrix}. \tag{7}$$

Noting that minimizing $\det(\mathbf{M}^{-1})$ is equivalent to maximizing $\det(\mathbf{M})$ we obtain the following problem formulation:

$$\begin{aligned} \max \quad & \det(\mathbf{M}) \\ \text{s.t.:} \quad & \mathbf{M} \geq 0, \\ & b_{\min} \leq b_i \leq b_{\max}, \quad i = 1, \ldots, N. \end{aligned} \tag{8}$$

2.2. Solutions to the D-Optimal Design Problem. The explicit form of the objective function of the optimization problem in (8) is

$$\det(\mathbf{M}) = N\sum_{i=1}^{N} b_i^2 - \left(\sum_{i=1}^{N} b_i\right)^2. \tag{9}$$

It can be seen that, in contrast to previous studies, the D-optimal design is independent of the unknown parameters. Thus, it can be used when imaging different organs as well as in other applications. For $N = 2$ the objective function becomes $\det(\mathbf{M}) = (b_1 - b_2)^2$. Therefore the D-optimal design is $b_1 = b_{\min}$, $b_2 = b_{\max}$. For $N = 3$ the objective function becomes $\det(\mathbf{M}) = (b_1 - b_2)^2 + (b_1 - b_3)^2 + (b_3 - b_2)^2$. Consequently, the D-optimal design is $b_1 = b_2 = b_{\min}$, $b_3 = b_{\max}$ or equivalently $b_1 = b_2 = b_{\max}$, $b_3 = b_{\min}$. Generally, one can see that for arbitrary N the D-optimal experiment design is obtained when

$$\begin{aligned} b_i &= b_{\min} \quad \forall i = 1, \ldots, n, \\ b_i &= b_{\max} \quad \forall i = n+1, \ldots, N, \end{aligned} \tag{10}$$

where $n = N/2$ if N is even; otherwise $n = (N+1)/2$. In the next section we compare the D-optimal design with the ED and GCRLB designs.

3. Evaluation and Simulation Results

In this section we evaluate the proposed D-optimal experiment design method and compare it with existing optimal design methods. We run Monte Carlo simulations using the pseudo-algorithm given in Appendix A. In our simulations we use the Rician noise distribution. While this does not match the noise assumptions of our theoretical framework, it permits a more realistic evaluation of the results for ADC imaging. We use the range $[0.1, 3] \times 10^{-3}$ mm^2/s of D values that are reported for human brain studies [4, 23]. In abdominal organs the range extends up to 5×10^{-3} mm^2/s [7]. In the text to follow we note that (i) the units associated with D and b have been omitted for readability (all b-values are stated in s/mm^2) and (ii) $E(x) = (1/N_{\mathrm{MC}}) \sum_{i=1}^{N_{\mathrm{MC}}} \hat{x}$. It is also noteworthy that we used LSE throughout the paper for parameter estimation.

3.1. Comparison to GCRLB. Given that the GCRLB method [23] is specifically designed for ADC estimation and is in good agreement with previous studies [21, 22], herein we compare the proposed D-optimal design with the GCRLB method. Figure 2 shows the standard deviation of estimated ADC values (σ_D) for a range of D values, where $N = 2$, $b_{\min} = 0$, $b_{\max} = 2000$, $m_0 = 500$, $N_{\mathrm{MC}} = 20000$, and SNR $= m_0/\sigma_G$. According to table 3 in [23] the optimal two-point design for $D \in [0.1, 3] \times 10^{-3}$ is $b_1 = 0$, $b_2 = 820$ while the D-optimal method suggests $b_1 = 0$, $b_2 = b_{\max}$. Several key observations can be drawn from Figure 2. (i) Increasing the SNR from 4 to 10 significantly improves the performance of the GCRLB. In addition, the performance of the GCRLB is heavily dependent on the D values to be measured. In contrast, the performance of the D-optimal design is very consistent, demonstrating robustness to changes in SNR and D. (ii) The D-optimal design outperforms the GCRLB over the entire range of D values and SNRs. (iii) For small D values and high SNR, where the Rician distribution can be fairly approximated by a Gaussian distribution [25], the performance of the GCRLB is close to that of the D-optimal design. (iv) Though the Rician noise model does not match our theoretical noise assumption, the precision of $\widehat{D}$ is independent of its actual value, D.

Figure 3 compares the GCRLB and D-optimal designs in terms of error (computed as $|E(\widehat{D}) - D|$) and standard deviation of $\widehat{D}$ (illustrated as vertical bars for each D value), where $N = 10$, $b_{\min} = 0$, $b_{\max} = 2000$, $m_0 = 500$, $N_{\mathrm{MC}} = 20000$, and SNR $= m_0/\sigma_G = 10$. According to table 3 in [23] the optimal ten-point design for $D \in [0.1, 3] \times 10^{-3}$ is $b_1 = b_2 = 0$, $b_3 = b_4 = \cdots = b_8 = 700$, and $b_9 = b_{10} = b_{\max}$ while the D-optimal design suggests $b_1 = \cdots = b_5 = 0$, $b_6 = \cdots = b_{10} = b_{\max}$. It can be seen in Figure 3 that the D-optimal design performs better in terms of accuracy and precision. Figure 4 shows, for the same test, plots of the bias (computed as $E(\widehat{m}_0) - m_0$) and standard deviation of $\widehat{m}_0$. It can be seen that the proposed method leads to both accurate and precise estimation of m_0. In addition, the D-optimal design shows very consistent performance over the whole range of D values. It is noteworthy that the GCRLB method severely underestimates m_0 for high D values.

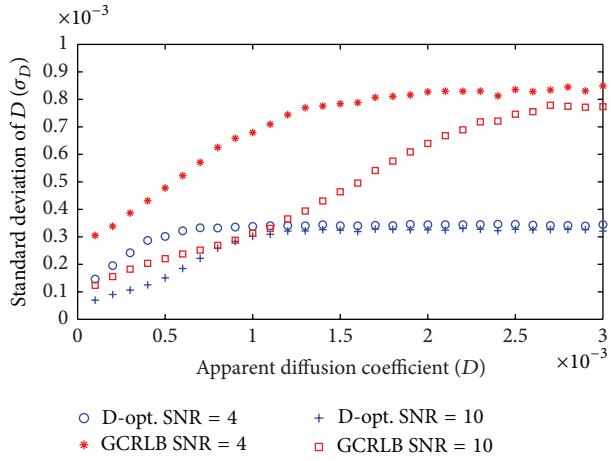

FIGURE 2: Standard deviation of estimated ADC values (σ_D) for a range of D values, where $N = 2$, $b_{\min} = 0$, $b_{\max} = 1500$, $m_0 = 500$, $N_{MC} = 20000$, and SNR = m_0/σ_G. The proposed D-optimal method is compared to GCRLB [23].

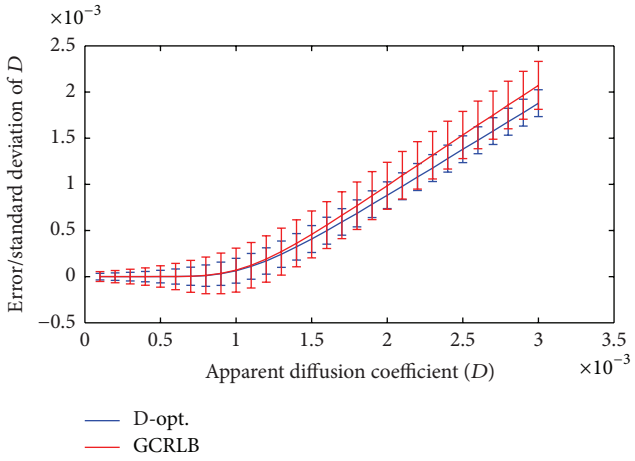

FIGURE 3: Error and standard deviation of estimated ADC values (vertical bars) for a range of D values, where $N = 10$, $b_{\min} = 0$, $b_{\max} = 1500$, $m_0 = 500$, $N_{MC} = 20000$, and SNR = $m_0/\sigma_G = 10$. The proposed D-optimal method is compared to GCRLB [23].

3.2. Sensitivity Analysis and Comparison to the ED Design. In this section we evaluate the sensitivity of the D-optimal design to changes in input parameters such as D, N, $b_{\max}$, and SNR. The input variable $b_{\min}$ is not considered because it is usually set to $b_{\min} = 0$.

The ADC value may vary depending on tissue type, pathological/developmental changes, and aging. The error and standard deviation of $\widehat{D}$ and $\widehat{m}_0$ are illustrated in Figure 5 for the range $D \in [0.1, 5] \times 10^{-3}$, where $N = 10$, $b_{\min} = 0$, $b_{\max} = 2000$, $m_0 = 500$, $N_{MC} = 20000$, and SNR = $m_0/\sigma_G = 10$. It can be seen that the D-optimal design outperforms the ED design in terms of accuracy and precision. Notably, the difference in estimation of m_0 is extremely large. This can have a significant impact on studies that use the diffusion signal itself as a biomarker (as in [14]). Note that, for the D-optimal design, the variance of σ_D is almost fixed for

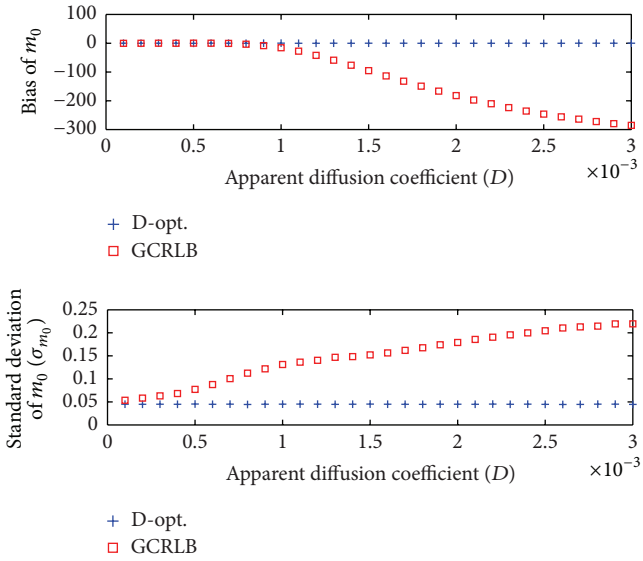

FIGURE 4: Bias and standard deviation of the estimated m_0 values for a range of D values, where $N = 10$, $b_{\min} = 0$, $b_{\max} = 1500$, $m_0 = 500$, $N_{MC} = 20000$, and SNR = $m_0/\sigma_G = 10$. The proposed D-optimal method is compared to GCRLB [23].

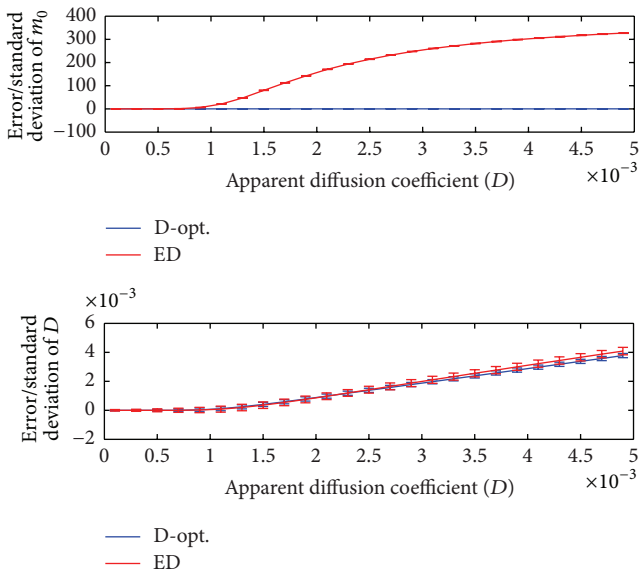

FIGURE 5: Error and standard deviation of $\widehat{D}$ and $\widehat{m}_0$ for the range $D \in [0.1, 5] \times 10^{-3}$, where $N = 10$, $b_{\min} = 0$, $b_{\max} = 2000$, $m_0 = 500$, $N_{MC} = 20000$, and SNR = $m_0/\sigma_G = 10$. The D-optimal design is compared to the ED design (where b_is are equidistantly distributed between $b_{\min}$ and $b_{\max}$).

$D \in [1, 5] \times 10^{-3}$. This consistency of performance is also apparent in the estimation of m_0.

The number of measurements is in general limited by the available clinical scan time. Here, we consider a range of N that is feasible for clinical studies according to the literature. The error and standard deviation of $\widehat{D}$ and $\widehat{m}_0$ are illustrated in Figure 6 for the range $N = 2$ to $N = 20$, where $D = 1 \times 10^{-3}$, $b_{\min} = 0$, $b_{\max} = 2000$, $m_0 = 500$, $N_{MC} = 20000$, and

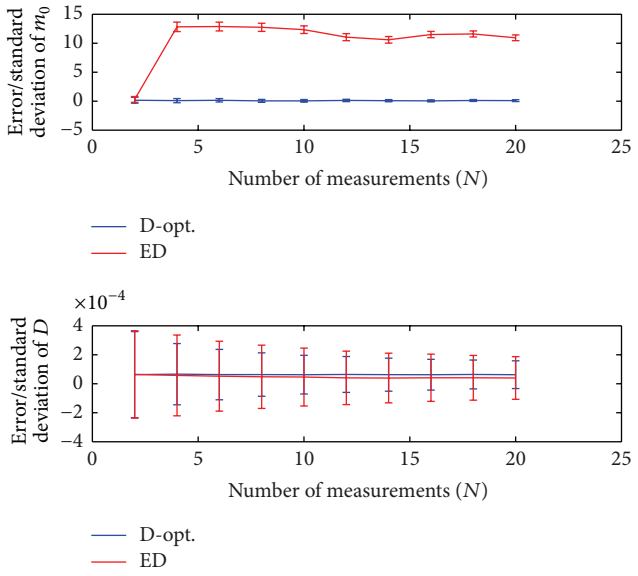

FIGURE 6: Error and standard deviation of $\widehat{D}$ and $\widehat{m}_0$ for the range $N = 2$ to $N = 20$, where D $= 1 \times 10^{-3}$, $b_{\min} = 0$, $b_{\max} = 2000$, $m_0 = 500$, $N_{\mathrm{MC}} = 20000$, and SNR $= m_0/\sigma_G = 10$. The D-optimal design is compared to the ED design.

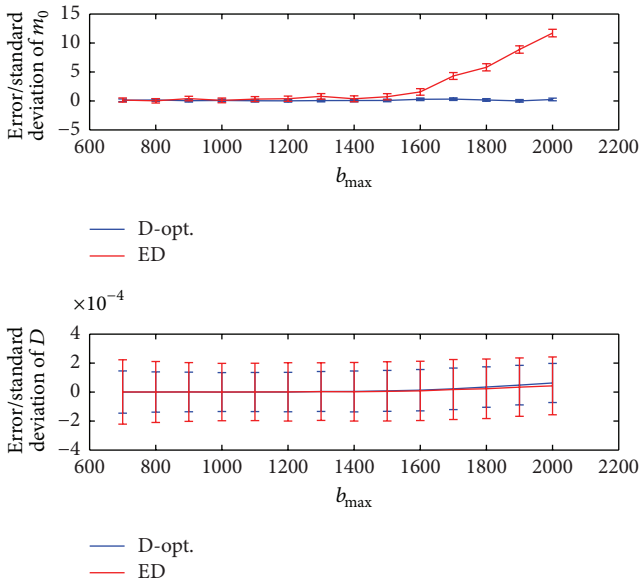

FIGURE 7: Error and standard deviation of $\widehat{D}$ and $\widehat{m}_0$ as a function of $b_{\max}$, where $D = 1 \times 10^{-3}$, $N = 10$, $b_{\min} = 0$, $m_0 = 500$, $N_{\mathrm{MC}} = 20000$, and SNR $= m_0/\sigma_G = 10$. The D-optimal design is compared to the ED design.

SNR $= m_0/\sigma_G = 10$. It shows that the D-optimal design outperforms the ED design in terms of standard deviation (vertical bars) of $\widehat{D}$ and $\widehat{m}_0$. As N increases, the variance of the estimated parameters decreases for both design methods while the accuracy is almost constant. Note that for $N = 2$ the two design methods lead to the same solution. Deviating from D-optimal solution, accuracy/precision of $\widehat{m}_0$ for the ED method considerably decreases even with higher number of measurements (cf. $N = 2$ with $N = 4$).

Different $b_{\max}$ values are recommended in the literature for different target organs/tissues. For example, [1] suggests $b_{\max} = 700$ for kidney while $b_{\max} = 1500$ is used for head and neck imaging [20] and $b_{\max} = 2000$ for brain imaging [18]. The error and standard deviation of $\widehat{D}$ and $\widehat{m}_0$ are illustrated in Figure 7 for the range $b_{\max} = 700, 800, \ldots, 2000$, where $D = 1 \times 10^{-3}$, $N = 10$, $b_{\min} = 0$, $m_0 = 500$, $N_{\mathrm{MC}} = 20000$, and SNR $= m_0/\sigma_G = 10$. It can be seen that the D-optimal design outperforms the ED design in terms of standard deviation (vertical bars) of $\widehat{D}$ and $\widehat{m}_0$. For the ED design, as $b_{\max}$ increases it does not make a considerable difference to the estimation of D but it does negatively impact on the estimation of m_0 producing increasingly larger errors for values of $b_{\max}$ beyond 1600. In contrast, the D-optimal design shows a better and relatively consistent performance over the whole range (with almost constant accuracy and precision).

The signal-to-noise ratio also affects the accuracy and precision of the estimation problem. We investigate the effect of SNR on the proposed experiment design as follows. The error and standard deviation of $\widehat{D}$ and $\widehat{m}_0$ are illustrated in Figure 8 as a function of SNR (defined as m_0/σ_G), where $D = 1 \times 10^{-3}$, $N = 10$, $b_{\min} = 0$, $b_{\max} = 2000$, $m_0 = 500$, and $N_{\mathrm{MC}} = 20000$. It shows that, over the whole range of SNR values, the

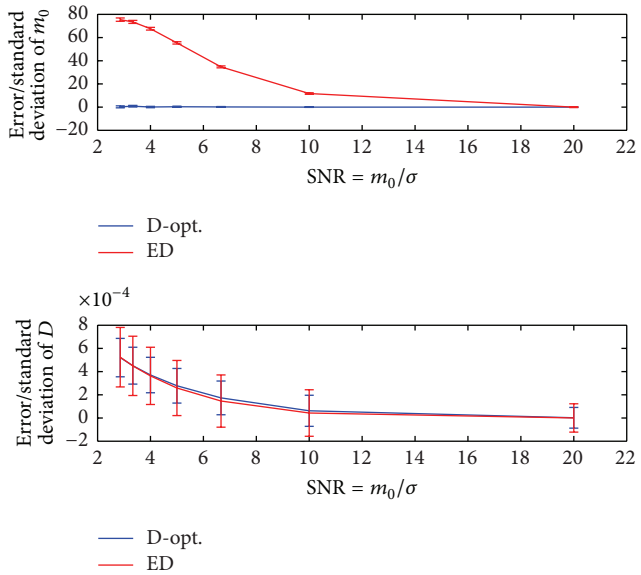

FIGURE 8: Error and standard deviation of $\widehat{D}$ and $\widehat{m}_0$ as a function of SNR (defined as m_0/σ_G), where $D = 1 \times 10^{-3}$, $N = 10$, $b_{\min} = 0$, $b_{\max} = 2000$, $m_0 = 500$, and $N_{\mathrm{MC}} = 20000$. The D-optimal design is compared to the ED design.

D-optimal design leads to minimum variance estimation of the unknown parameters. For ED design, the accuracy and precision of both $\widehat{D}$ and $\widehat{m}_0$ improve with increasing SNR while for the D-optimal design an improvement is only seen for $\widehat{D}$.

3.3. Tests on a Mean Diffusivity Map. To illustrate the impact that experiment design may have on diffusion-weighted

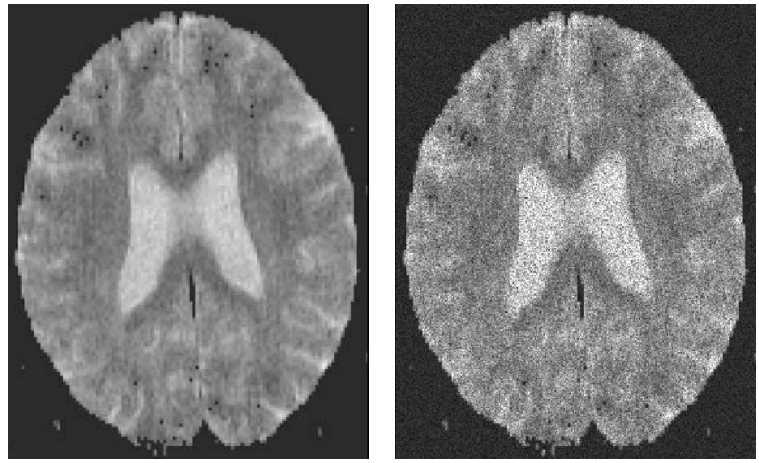

(a) (b)

Figure 9: Original mean diffusivity map considered as ground truth (a) and an example noisy image produced by adding Rician distributed noise, where SNR = 5 (b). The original image is taken from [18].

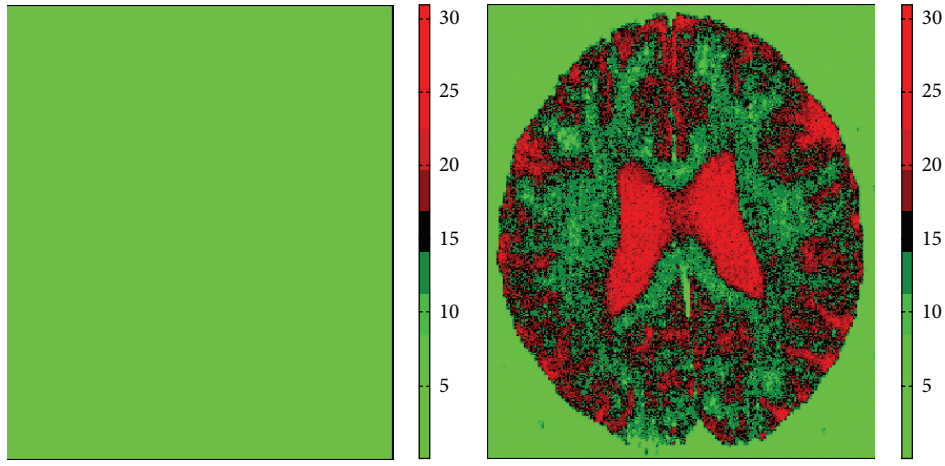

(a) (b)

Figure 10: Error in estimation of diffusion signal computed as $|E(\widehat{m}_0) - m_0|$ for the D-optimal (a) and ED (b) design methods. The color bar ranges from 0 to 31.

images, we perform the following test. We take figure 4.(a) in [18] as the ground truth image. Then we add Rician distributed noise pixelwise (SNR = 5). The original image and an example of noisy images are shown in Figure 9.

Let $I(i, j)$ denote a pixel intensity in the original image. Then we run Algorithm 1 with the following setting for all pixels: $m_0 = I(i, j)$, SNR $= m_0/5$, $N = 20$, $D = 1 \times 10^{-3}$, $b_{\text{min}} = 0$, $b_{\text{max}} = 2000$, and $N_{\text{MC}} = 20000$. The resultant images computed as error in estimation of $\widehat{m}_0$ ($|E(\widehat{m}_0) - m_0|$) and its standard deviation are shown in Figures 10 and 11, respectively. Figure 10 shows that one can accurately estimate diffusion signal using the D-optimal design. The accuracy is almost independent of the signal level. In contrast, the ED design produces large errors for high signal levels. In applications that consider statistics in small ROIs (such as [11]) this may be misleading.

The optimal experiment design is fundamentally based on improving the precision of the estimation problem. This can be seen in Figure 11, where we illustrate the standard deviation of $\widehat{m}_0$. It can be seen that the D-optimal design consistently produces lower variance than the ED design. It is noteworthy that Figures 10 and 11 represent the sensitivity analysis with respect to m_0 and confirm the stable performance of the D-optimal design.

4. Discussions

Although the current work focuses on ADC imaging, the proposed method can be applied in experiment design for other applications of the monoexponential model. As an example, empirical evaluations in [17] show that adding more measurements on b_{min} improves the results of model fitting

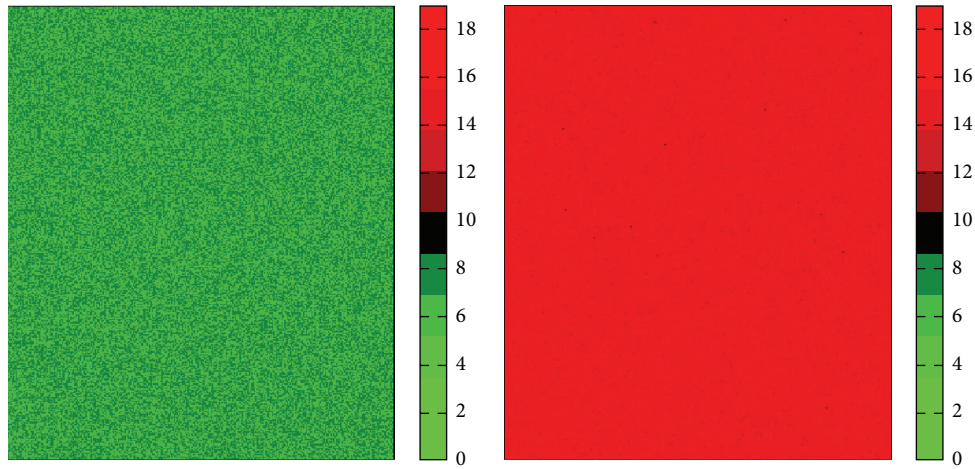

(a) (b)

Figure 11: Standard deviation in estimation of $\widehat{m}_0$. The D-optimal design (a) produces more precise estimates compared to the ED design (b). Note that the standard deviation is multiplied by 100 to enhance the visualization.

Data: D, m_0, N, $b_{\min}$, $b_{\max}$, σ_G and N_{MC}, number of Monte Carlo trials.
Result: Mean value and standard deviation of $\widehat{D}$ and $\widehat{m}_0$
(i) Choose an algorithm ED/GCRLB/D-opt. to assign b_i $\forall i = 1, \ldots, N$.
(ii) Set $m_i = m_0 \exp(-b_i D)$.
for $r = 1$ **to** N_{MC} **do**
(i) Add Rician distributed noise to m_is to obtain SNR $= m_0/\sigma_G$;
(ii) Compute the unknown parameters $\widehat{D}$ and $\widehat{m}_0$;
(iii) Record the mean value and standard deviation of $\widehat{D}$ and $\widehat{m}_0$.

Algorithm 1: Pseudo-algorithm to evaluate an experiment design.

in enzyme kinetics (compared to the ED design). This is in agreement with our findings.

Comparing the proposed method to previous studies, we see that it (i) is based on less restrictive noise assumptions and thus covers a wider range of applications, (ii) shows that the optimal design is not necessarily dependent on the imaged parameters, (iii) outperforms the ED and GCRLB methods (based on evaluations using simulated data), and (iv) is applicable even if the noise assumptions are partly violated.

Figures 3 and 5 show that (i) in contrast to the findings in [23] there exist D-independent optimal designs that minimize variance of the estimated ADC values and (ii) even using optimal designs D values greater than 1.1×10^{-3} cannot be estimated accurately. In other words, the error of $\widehat{D}$ is larger than 10% when $D > 1.1 \times 10^{-3}$. This means that ADC values reported for cartilage, muscle [23], and normal white matter [4] are accurate/reliable while high ADC values reported for normal kidney [7] should arguably be treated with caution. This warrants further investigation using real data.

Noise Distribution. The noise assumptions (independency and equal variance) are necessary for tractable theoretical derivations but do not necessarily limit the proposed method to Gaussian noise. For example, these assumptions hold for scenarios with independent but nonidentical noise distributions provided that they have equal variances. We have evaluated the proposed method in realistic cases (independent Rician noise with nonequal variances). However, in modern scanners with phased arrays and multicoil acquisition [26], the noise is noncentrally χ-distributed [27]. The D-optimal design problem for such kind of noise distributions is intractable. In addition, relaxing the *"equal variance"* condition, the D-optimal design becomes dependent on the imaged parameters. Thus, we can not find an optimal design that performs well over the whole range of the imaged parameters.

Estimation Method. One can use other estimation methods instead of LSE. Possibilities include the median estimator [18], maximum likelihood estimator (MLE), and weighted least squares (WLS) [28]. The exact formulation of the D-optimal design problem for these estimation techniques is dependent on the noise distribution and often becomes intractable. In the case of Gaussian noise the MLE leads to the same solution as LSE.

Physical Considerations. Given that the proposed method takes the minimum and maximum b-values as the input, one can adjust the range to avoid the signal distortion caused by physical phenomena such as the perfusion effect at low b-values and non-Gaussian behavior at high b-values.

5. Conclusion

The need for precise estimation of biomedical quantities has given rise to studies concerning optimal experiment design for monoexponential model fitting. In this paper, we formulated the problem as a D-optimal design problem that is a convex optimization problem. In contrast to previous studies, we did not restrict our theoretical framework to model fitting in the presence of Gaussian noise. Solving this problem and evaluating the results for ADC imaging on simulated data, we showed that the optimal design is independent of the imaged parameters. Furthermore, Monte Carlo simulations showed that the D-optimal design outperforms the ED and GCRLB methods. Moreover the proposed method is applicable to a wider range of problems because of its less restrictive noise assumptions. Our evaluations show that it is applicable even if the noise assumptions are partly violated. An important practical result is that accurate estimation of high ADC values is not possible even using optimal experiment design.

Appendices

A. Evaluation of an Experiment Design

Here we provide a pseudo-code for the algorithm used in Section 3 (see Algorithm 1).

B. GCRLB Experiment Design

In an estimation problem, the lower bound of the variance of a parameter x_j, $\sigma^2(x_j)$, is given by the corresponding diagonal element of the inverse of the Fisher information matrix:

$$\sigma^2\left(x_j\right) \geq \left(\mathbf{F}^{-1}\right)_{jj}. \tag{B.1}$$

This is known as the Cramer-Rao lower bound (CRLB). Assuming zero-mean Gaussian noise on m in (1), one can obtain the following Fisher information matrix for ADC imaging [23]:

$$\mathbf{F} = \frac{1}{\sigma_G}\begin{bmatrix} \sum_{i=1}^{N} \exp\left(-2b_iD\right) & -\sum_{i=1}^{N} b_iS_0 \exp\left(-2b_iD\right) \\ -\sum_{i=1}^{N} b_iS_0 \exp\left(-2b_iD\right) & \sum_{i=1}^{N} b_i^2S_0^2 \exp\left(-2b_iD\right) \end{bmatrix}. \tag{B.2}$$

In the derivation above $\mathbf{x} = [S_0 \quad D]$. The GCRLB experiment design entails minimizing the CRLB of D, $(\mathbf{F}^{-1})_{22}$, with respect to b_is for a given value/range of D. The reader is referred to [23] for more details.

Conflict of Interests

The authors declare that there is no conflict of interests regarding the publication of this paper.

References

[1] D. M. Koh and H. C. Thoeny, *Diffusion-Weighted MR Imaging: Applications in the Body*, Springer, Berlin, Germany, 2010.

[2] E. Sjögren, H. Lennernäs, T. B. Andersson, J. Gråsjö, and U. Bredberg, "The multiple depletion curves method provides accurate estimates of intrinsic clearance (CL_{int}), maximum velocity of the metabolic reaction (V_{max}), and michaelis constant (K_m): accuracy and robustness evaluated through experimental data and monte carlo simulations," *Drug Metabolism and Disposition*, vol. 37, no. 1, pp. 47–58, 2009.

[3] R. Urso, P. Blardi, and G. Giorgi, "A short introduction to pharmacokinetics," *European Review for Medical and Pharmacological Sciences*, vol. 6, no. 2, pp. 33–44, 2002.

[4] R. N. Sener, "Diffusion MRI: apparent diffusion coefficient (ADC) values in the normal brain and a classification of brain disorders based on ADC values," *Computerized Medical Imaging and Graphics*, vol. 25, no. 4, pp. 299–326, 2001.

[5] W. Abdulghaffar and M. M. Tag-Aldeen, "Role of diffusion-weighted imaging (DWI) and apparent diffusion coefficient (ADC) in differentiating between benign and malignant breast lesions," *The Egyptian Journal of Radiology and Nuclear Medicine*, vol. 44, no. 4, pp. 945–951, 2013.

[6] J.-M. Shen, X.-W. Xia, W.-G. Kang, J.-J. Yuan, and L. Sheng, "The use of MRI apparent diffusion coefficient (ADC) in monitoring the development of brain infarction," *BMC Medical Imaging*, vol. 11, article 2, 2011.

[7] J. L. Zhang, E. E. Sigmund, H. Chandarana et al., "Variability of renal apparent diffusion coefficients: limitations of the monoexponential model for diffusion quantification," *Radiology*, vol. 254, no. 3, pp. 783–792, 2010.

[8] C. Göya, C. Hamidi, Y. Bozkurt et al., "The role of apparent diffusion coefficient quantification in differentiating benign and malignant renal masses by 3 Tesla magnetic resonance imaging," *Balkan Medical Journal*, vol. 32, no. 3, pp. 273–278, 2015.

[9] S. Emad-Eldin, M. Halim, L. I. A. Metwally, and R. M. Abdel-Aziz, "Diffusion-weighted MR imaging and ADC measurement in normal prostate, benign prostatic hyperplasia and prostate carcinoma," *The Egyptian Journal of Radiology and Nuclear Medicine*, vol. 45, no. 2, pp. 535–542, 2014.

[10] M. A. Jacobs, R. Ouwerkerk, K. Petrowski, and K. J. MacUra, "Diffusion-weighted imaging with apparent diffusion coefficient mapping and spectroscopy in prostate cancer," *Topics in Magnetic Resonance Imaging*, vol. 19, no. 6, pp. 261–272, 2008.

[11] N. Mukuda, S. Fujii, C. Inoue et al., "Apparent diffusion coefficient (ADC) measurement in ovarian tumor: effect of region-of-interest methods on ADC values and diagnostic ability," *Journal of Magnetic Resonance Imaging*, 2015.

[12] K. A. Ahmad and A. Abdrabou, "The significance of added ADC value to conventional MR imaging in differentiation between benign and malignant ovarian neoplasms," *The Egyptian Journal of Radiology and Nuclear Medicine*, vol. 45, no. 3, pp. 997–1002, 2014.

[13] K. Tsukamoto, E. Matsusue, Y. Kanasaki et al., "Significance of apparent diffusion coefficient measurement for the differential diagnosis of multiple system atrophy, progressive supranuclear

palsy, and Parkinson's disease: evaluation by 3.0-T MR imaging," *Neuroradiology*, vol. 54, no. 9, pp. 947–955, 2012.

[14] Y. Lei, H. Wang, H.-F. Li et al., "Diagnostic significance of diffusion-weighted MRI in renal cancer," *BioMed Research International*, vol. 2015, Article ID 172165, 12 pages, 2015.

[15] A. Ogura, K. Hayakawa, T. Miyati, and F. Maeda, "Imaging parameter effects in apparent diffusion coefficient determination of magnetic resonance imaging," *European Journal of Radiology*, vol. 77, no. 1, pp. 185–188, 2011.

[16] T. Yoshikawa, H. Kawamitsu, D. G. Mitchell et al., "ADC measurement of abdominal organs and lesions using parallel imaging technique," *American Journal of Roentgenology*, vol. 187, no. 6, pp. 1521–1530, 2006.

[17] E. Sjögren, J. Nyberg, M. O. Magnusson, H. Lennernäs, A. Hooker, and U. Bredberg, "Optimal experimental design for assessment of enzyme kinetics in a drug discovery screening environment," *Drug Metabolism and Disposition*, vol. 39, no. 5, pp. 858–863, 2011.

[18] A. Kristoffersen, "Diffusion measurements and diffusion tensor imaging with noisy magnitude data," *Journal of Magnetic Resonance Imaging*, vol. 29, no. 1, pp. 237–241, 2009.

[19] J. Yuan, D. K. W. Yeung, G. S. P. Mok et al., "Non-Gaussian analysis of diffusion weighted imaging in head and neck at 3T: a pilot study in patients with nasopharyngeal carcinoma," *PLoS ONE*, vol. 9, no. 1, Article ID e87024, 2014.

[20] J. F. A. Jansen, H. E. Stambuk, J. A. Koutcher, and A. Shukla-Dave, "Non-gaussian analysis of diffusion-weighted MR imaging in head and neck squamous cell carcinoma: a feasibility study," *American Journal of Neuroradiology*, vol. 31, no. 4, pp. 741–748, 2010.

[21] Y. Bito, S. Hirata, and E. Yamamoto, "Optimum gradient factors for apparent diffusion coefficient measurements," in *Proceedings of the SMR/ESMRMB Joint Meeting*, p. 913, Nice, France, August 1995.

[22] D. Xing, N. G. Papadakis, C. L.-H. Huang, V. M. Lee, T. A. Carpenter, and L. D. Hall, "Optimised diffusion-weighting for measurement of apparent diffusion coefficient (ADC) in human brain," *Magnetic Resonance Imaging*, vol. 15, no. 7, pp. 771–784, 1997.

[23] O. Brihuega-Moreno, F. P. Heese, and L. D. Hall, "Optimization of diffusion measurements using Cramer-Rao lower bound theory and its application to articular cartilage," *Magnetic Resonance in Medicine*, vol. 50, no. 5, pp. 1069–1076, 2003.

[24] J. J. Ye and J. Zhou, "Minimizing the condition number to construct design points for polynomial regression models," *SIAM Journal on Optimization*, vol. 23, no. 1, pp. 666–686, 2013.

[25] M. Björk, *Contributions to signal processing for MRI [Ph.D. thesis]*, Uppsala University, 2015.

[26] C. D. Constantinides, E. Atalar, and E. R. McVeigh, "Signal-to-noise measurements in magnitude images from NMR phased arrays," *Magnetic Resonance in Medicine*, vol. 38, no. 5, pp. 852–857, 1997.

[27] J. Veraart, J. Rajan, R. R. Peeters, A. Leemans, S. Sunaert, and J. Sijbers, "Comprehensive framework for accurate diffusion MRI parameter estimation," *Magnetic Resonance in Medicine*, vol. 70, no. 4, pp. 972–984, 2013.

[28] J. Veraart, J. Sijbers, S. Sunaert, A. Leemans, and B. Jeurissen, "Weighted linear least squares estimation of diffusion MRI parameters: strengths, limitations, and pitfalls," *NeuroImage*, vol. 81, pp. 335–346, 2013.